

Optimal Design of a Sustainable Extraction Process for the Treatment of Acidic Wastewater

Zhe Li^a, Xue Wang^a, Wende Tian^{a,*}, Dongwu Sui^b

^aCollege of Chemical Engineering, Qingdao University of Science & Technology, 266042 Qingdao, China

^bWanhua Chemical Group Co., Ltd., 264002, Yantai, China
 tianwd@qust.edu.cn

The wastewater from the fluid catalytic cracking refinery is difficult to treat because of its high organic and oil content. A sustainable extraction process is designed to treat the wastewater. In this process, oil is first separated from wastewater to facilitate further removal of phenol from wastewater. The purification process of oil phase makes use of parazole to extract phenol from oil and wastewater to back-extract parazole, while the purification process of water phase makes use of Methyl Butyl Ketone (MBK) to extract phenol from wastewater followed by distillation recycling of MBK. The extraction mechanism is explained by molecular simulation from micro-level. Compared to traditional extraction operations, this treatment process reduces the make-up of extractant greatly and is sustainable. Subsequently, the extraction process is optimised by sensitivity analysis and Heat Integration with Aspen Plus software. The simulation result exhibits high purity of disposed oil and wastewater (up to 99.50 % and 99.99 %) and a great reduction of energy consumption, utility cost, and CO₂ emission. Finally, one control scheme is designed for this process after its anti-disturbance ability is verified with Aspen Dynamics software.

1. Introduction

Acidic wastewater from fluid catalytic cracking (FCC) refinery accounts for a large part of industrial wastewater discharge (Wang et al., 2019). As acidic wastewater is difficult to purify and recover, it is of great significance to design new treatment process in practice. The design of extraction process is the research hotspot. Jiao et al. (2015) designed a new extractant composed of imidazole and its homolog compounds for the separation of phenols from coal tar. Cui et al. (2018) proposed extraction of phenols from wastewater by employing internally synthesized extractant, with several possible schemes simulated by Aspen Plus software. Guo et al. (2019) presented a phenol extraction process by using the best designed solvent mixture. Sustainable process refers to the process with material recycling (Li et al., 2014) or energy reuse (Kiss, 2019) to achieve sustainable evolution. For example, Tian et al. (2019) proposed an optimised bipolar membrane electro dialysis strategy to dispose of industrial wastewater with solar energy for reducing the capital and operational costs. Cui et al. (2017) improved the wastewater treatment process through the Heat Integration of solvent recovery system to reduce the cost of wastewater treatment. It is of great significance to design a sustainable wastewater treatment process concerning the operation cost and the treatment effect simultaneously (Zhang et al., 2017). In this paper, a sustainable process removing oil and phenol from wastewater is designed by extraction operation. The main contribution of this work consists in the effective treatment of wastewater along with the balanced capital and operational costs, in which the extraction mechanism of the extractant is analysed from the micro-level to facilitate extractant selection.

2. Design of wastewater treatment process

The schematic diagram of FCC acid wastewater treatment is shown in Figure 1. The 130 t/h wastewater mainly consisting of 3.55 g/L phenol and 7.33 g/L oil enters the oil-water separator (V101) at normal temperature and pressure. It is separated into upper oil phase (OIL) and lower water phase (WA). Phenol is easily soluble in oil, so OIL contains a certain amount of phenol. OIL is passed into the extraction column

(T201) to separate phenol from oil by pyrazole as an extractant. The top discharge of T201 is oil while the bottom one is a mixture of phenol and pyrazole. Because pyrazole is soluble in water but phenol is not, one part of the WA stream is selected as the back-extraction agent to realise the recycle of pyrazole in column T203. The other part of WA enters the extraction column (T202) through the diverter FSPLIT. The Methyl Butyl Ketone (MBK) enters the bottom of T202 to separate phenol from wastewater by countercurrent extraction. The stream Mixture2, a mixture of MBK and phenol, is discharged from the top of T202 and goes into the distillation column (T301) to realise the subsequent separation. Extractant obtained from the top of T301 is blended with fresh extractant in the mixer MIX3, and then enters T202. Crude phenol outflows from the bottom of T301 at the same time. The treated wastewater effluent at the bottom of T202 is further treated by distillation column (T302) since it still contains a small amount of extractant. The analysis of this wastewater treatment effect is shown in Table 1.

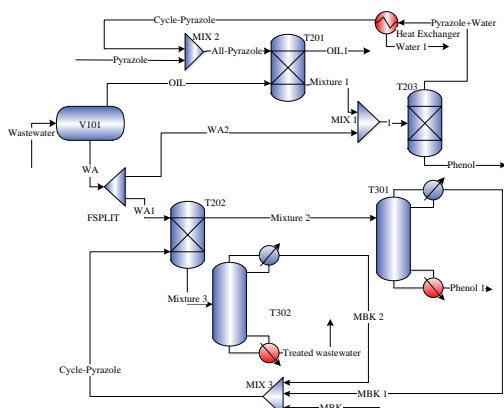


Figure 1: Schematic diagram of FCC acid wastewater treatment

Table 1: Effect of wastewater treatment

	Mass flow (kg/h)		Mass fractions	
	Treated oil	Treated wastewater	Treated oil	Treated wastewater
C ₆ H ₆ O	3.693	6.654	3.875×10^{-3}	5.177×10^{-5}
H ₂ O	2.894×10^{-5}	128,500	3.037×10^{-8}	99.995×10^{-2}
C ₈ H ₁₈	948.313	1.276×10^{-8}	99.505×10^{-2}	9.928×10^{-14}
Extractant	1.027	3.407×10^{-15}	1.077×10^{-3}	2.651×10^{-20}

It can be seen from Table 1 that the mass fraction of oil in the treated oil is 99.505 %, the mass concentration of the oil is 713.554 g/L (calculated as mole flow divided by volume flow), and the extraction ratio of phenol is 97.749 % (calculated as the mass of extracted substance divided by its total mass). The mass fraction of water in this treated wastewater is 99.995 %, and the phenol removal rate is 98.657 %. The recovery and utilization rate of the extractant is 91.906 % (calculated as the amount of circulating extractant divided by the amount of make-up extractant). The process well realises the removal of oil and phenol from the wastewater, while meeting the requirements of cyclic utilization of the extractant. It achieves the demand of “waste control by waste” since the wastewater is also used as the back-extractant without introducing new extractant. It is a sustainable process with recycling of substances and wastewater.

3. Microscopic explanation of extraction mechanism

The Molclus and MOPAC (Zheng et al., 2016) programs in Gaussian09 software are used to analyse the interaction of the extractant and phenol at B3LYP/6-311G(d,p) level and provide zero correction energy. The interaction energy under the basis set superposition error (BSSE) correction is calculated at the B3LYP/6-311++G(d,p) level. The calculation results show that interaction energy of pyrazole and phenol under BSSE is -10.75 kcal/mol, and that of MBK and phenol is -10.32 kcal/mol. There is no covalent bond between the two extractants and the extracted material as their interaction energies are less than 100 kcal/mol (Filipek and Fortenberry, 2016).

Reduced density gradient analysis (RDG) can visualize weak interactions such as Van Der Waals Forces, hydrogen bonds, and steric repulsion in the system. The “atoms in molecules (AIM)” theory of Bader based on

the electron distribution analysis is a powerful tool to detect and characterize hydrogen bonds. The interaction forces of pyrazole and phenol, MBK and phenol are analysed by RGD and AIM, as shown in Figures 2 and 3.

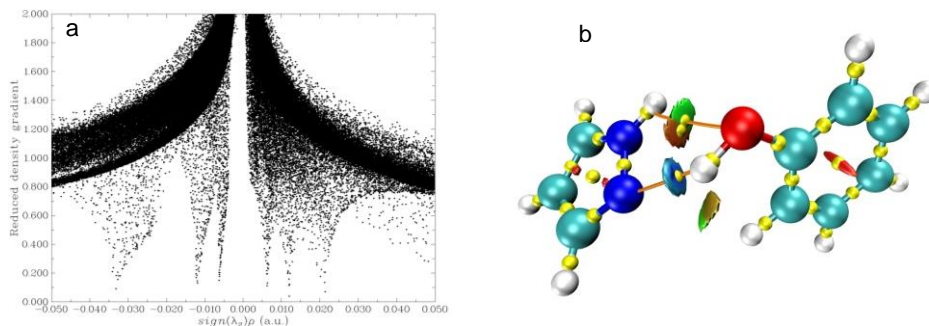


Figure 2: RGD and AIM of pyrazole and phenol

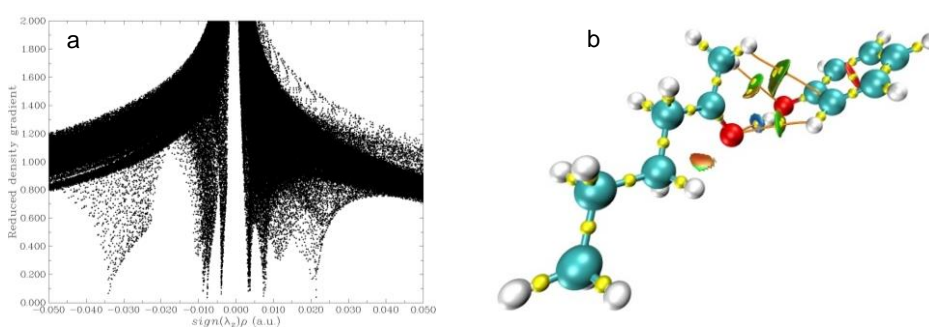


Figure 3: RGD and AIM of MBK and phenol

In Figures 2 and 3, “a” represents the RDG diagram and “b” represents the AIM diagram. It can be seen from Figure 2a that there is a spike between pyrazole and phenol in the region from -0.035 to -0.03 a.u. on the abscissa. According to the AIM theory, the electron density at the critical point of the hydrogen bond is -0.002-0.037 a.u., and the Laplace density ($\nabla^2\rho_{\text{BCP}}$) is 0.024-0.139. It can be concluded that a hydrogen bond exists between the pyrazole and phenol. In Figure 2b, the blue region corresponds to the left spike of the scatter plot, which is manifested as the strong N-HO hydrogen bond between nitrogen atom and phenol hydroxyl group. The green and brown regions correspond to the spike in the middle of the scatter plot, which is manifested as the weak interaction, mainly as Van Der Waals Force. The red fusiform region in the middle of the benzene ring and pyrazole five-membered ring corresponds to the rightmost spike of the scatter plot, which is reflected by the strong steric effect. Since the bond path and the bond critical point exist between pyrazole and phenol, the hydrogen bond size is then analysed. The hydrogen bond energy between O12H13-N17 is -35.106 kJ/mol, and that of N18H19-O12 is -11.295 kJ/mol. The interaction between pyrazole and phenol is dominated by OH-N hydrogen bond. While the strong hydrogen bond gives the extractant a better extraction effect, the NH-O hydrogen bond as an auxiliary hydrogen bond also contributes to the good extraction effect of pyrazole. Similarly, the analysis of Figure 3a and b show that the hydrogen bond energy between O22H23-O10 is the largest, which value is -37.083 kJ/mol. So the interaction energy between MBK and phenol representing the extraction ability of extractant is dominated by OH-O hydrogen bond. The bond energies of C1H3-O22 and C13H19-O10 hydrogen bonds are -7.887 kJ/mol and -6.224 kJ/mol, so the CH-O hydrogen bond as an auxiliary hydrogen bond also contributes to the good extraction effect of MBK.

4 Optimisation and control of wastewater treatment process

In the design specification, the mass fraction of water in the treated wastewater is set to 99.995×10^{-2} , and that of phenol in Phenol1 is 1.000. The sensitivity analysis is performed as follows.

4.1 Process optimisation and control

The optimisation proceeds in two directions. One is the optimisation of process decision variables, the other is heat transfer between streams through Heat Integration. For decision variables optimisation, the relationship between the number of stage and the heat duty of distillation column is first analysed, as shown in Figure 4.

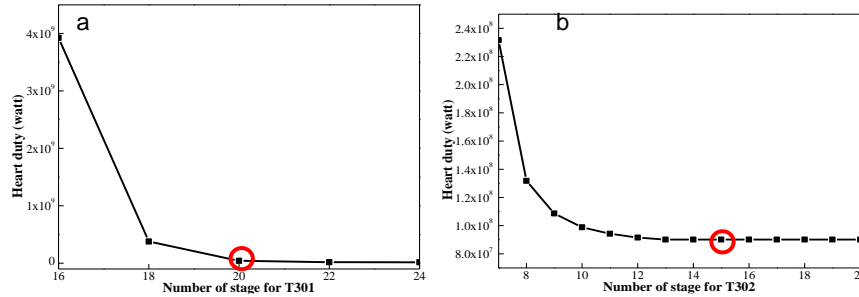


Figure 4: The influence of number of stage on the heat duty of T301 and T302

As shown in Figure 4a, increasing the number of stage can reduce the heat duty of distillation column, but also raise equipment investment cost. When the number of stage is greater than 20, the heat duty decrease is not obvious with the stages number up, so the number of stage of T301 is set to 20 to compromise the equipment investment costs as low as possible. Similarly, the number of stage of T302 is set to 13. Based on above results, the relationship between the feed stage and the heat duty is analysed in Figure 5.

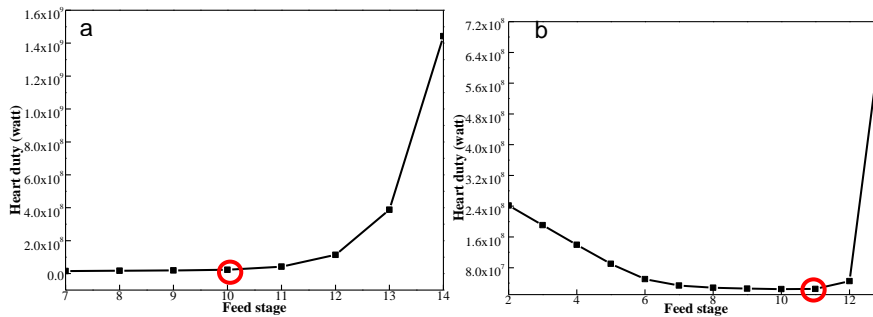


Figure 5: The influence of feed stage on the heat duty of T301 and T302

Figure 5a shows that the heat duty of T301 reaches the minimum when the 10th stage is set as feed stage. Similarly, feed is given to the 10th stage of T302 in Figure 5b. The relationship between the feed temperature and the heat duty is further analysed, as shown in Figure 6.

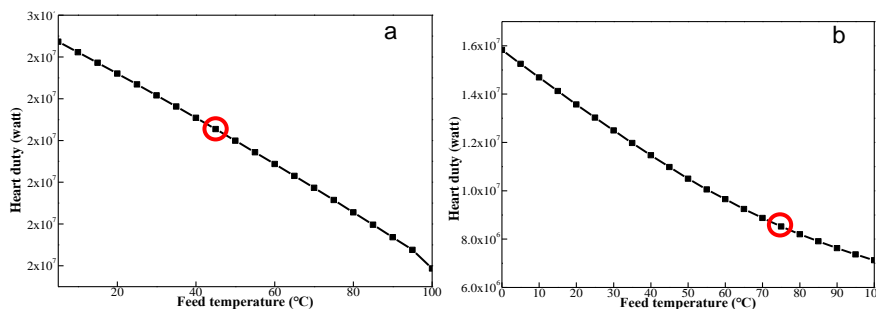


Figure 6: The influence of feed temperature on the heat duty of T301 (a) and T302 (b)

In Figure 6, the heat duty of distillation column decreases as feed temperature increases. Considering the properties of materials and the heat exchange capacity of cold and hot streams in this process, the feed temperature of T301 is set to 45 °C and that of T302 is 70 °C. Changing streams temperature through utilities will not only increase operational cost but also increase CO₂ emissions. This process is optimised by the heat exchange between streams. The optimised steady-state process is then imported into dynamics in pressure-driving pattern. The parameters including liquid level, temperature, product mole flow and product mass fraction are analysed by changing the feed flowrate. Some target controllers are added according to the trend of parameter changes, as shown in Figure 7. The control objective is to make the process maintain a controlled and safe production state under the disturbance.

In Figure 7, the process optimisation is achieved by adding heat exchangers. The T302 product stream is used to heat T301 feed to reduce the supply of thermal utilities. Using treated wastewater 2 to heat the feed of T302 not only reduces utility consumption but also decreases the temperature of treated wastewater. The

bottom product of T301 is used to heat the top stream of T302, which also decreases the temperature of product phenol and the amount of thermal utility.

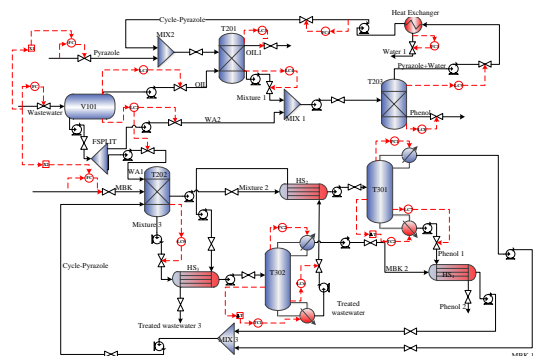


Figure 7: Sustainable wastewater treatment process optimisation and control.

The optimised process realises the heat exchange between streams without changing the treatment effect, reduces the emission of CO₂, and further the energy consumption and cost, as shown in Table 2.

Table 2: Effect of process optimisation

	Before optimisation		After optimisation	
	T301	T302	T301	T302
Heat duty (kW)	2.360×10 ⁴	13,570	20,860	10,980
Utility cost (\$/h)	212.400	92.808	187.776	75.096
CO ₂ emission (kg/h)	5,586	3,212	4,938	2,599

According to Table 2, the heat duty after optimisation is reduced by 5,330 kW, the cost of utilities is reduced by 42.336 \$/h, and the CO₂ emission is reduced by 1,261 kg/h. As the flow of wastewater in production, phenol concentration and other conditions may fluctuate due to different operations, dynamic simulation of this process will be further carried out to analyse the stability of this process in the face of feed disturbance.

4.2 Analysis of dynamic simulation

The level, flow, temperature and proportional controllers are added to the flowsheet given in Figure 7. The control effect of process is shown in Figure 8.

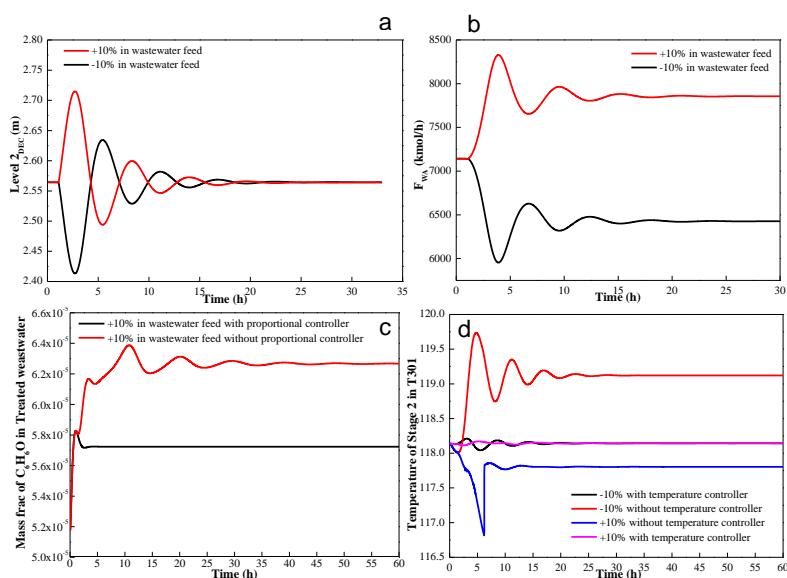


Figure 8: Process variation after changing the feed flow under different controllers

Figure 8 shows the change of each parameter when changing 10 % of wastewater feed in one hour. Figure 8a depicts the change of the liquid level of V101. It can be seen that the liquid level recovers to a normal range after a slight fluctuation when adding a liquid level controller. Figure 8b depicts the change of the discharge WA of V101. For the feed flow changes by 10 %, the discharge amount also changes to a certain extent, and gradually becomes stable. The control effect of the proportional controller is given in Figure 8c. Compared with the process without proportional controller, the phenol contents in the treated wastewater changes little and the speed of returning to normal value is faster. By comparing the changes with and without temperature controller in Figure 8d, it is proved that the temperature change of T301 is small after adding the temperature controller, and the speed of returning to the normal value is faster. The safety and efficiency of the designed process are guaranteed.

5. Conclusions

The process established by Aspen Plus software realises the extractant reuse without introducing new back-extractant, and reaches the sustainability aim. The extraction mechanism is analysed by Gaussian software. It can be obtained that the strong hydrogen bond between extractants and phenol makes extractants exhibit a better extraction effect, and other hydrogen bonds acting as an auxiliary hydrogen bond also contributes to the good extraction effect. This process is optimised through the heat exchange between streams. The optimisation results show that the mass fraction of oil in the treated oil is 99.505 % and the extraction ratio of phenol in the oil is 97.749 %. The mass fraction of water in this treated wastewater is 99.995 % and the phenol removal rate is 98.657 %. The heat duty after optimisation is reduced by 5,330 kW. The cost of utilities is reduced by 42.336 \$/h. The CO₂ emission is reduced by 1,261 kg/h. The optimised process improves the economy greatly while ensuring the treatment effect. Dynamic simulation is used to check the safety and stability of this process. After adding controllers, this process shows stable performance in the face of possible parameter changes. This paper focuses on the treatment of acidic wastewater, also applicable to other acidic wastewater. In this work, the economic feasibility and multi-parameter effects are not involved. In the future work, the economic feasibility of process and the common influence of multiple parameters will be considered.

Acknowledgements

The authors gratefully acknowledge that this work is supported by the National Natural Science Foundation of China (Grant No. 21576143).

References

- Cui P.Z., Mai Z.H., Yang S.Y., Qian Y., 2017, Integrated treatment processes for coal-gasification wastewater with high concentration of phenol and ammonia, *Journal of Cleaner Production*, 142, 2218-2226.
- Cui Z., Tian W.D., Qin H., Wang X., Zhao W.Y., 2018, Optimal design and control of Eastman organic wastewater treatment process, *Journal of Cleaner Production*, 198, 333-350.
- Filipek G.T., Fortenberry R.C., 2016, Formation of potential interstellar noble gas molecules in gas and adsorbed phases, *ACS Omega*, 1(5), 765-772.
- Guo C., Cao Q., Chen B.K., Yang S.Y., Qian Y., 2019, Development of synergistic extraction process for highly efficient removal of phenols from coal gasification wastewater, *Journal of Cleaner Production*, 211, 380-386.
- Jiao T.T., Li C.S., Zhuang X.L., Cao S.S., Chen H.N., Zhang S.J., 2015, The new liquid-liquid extraction method for separation of phenolic compounds from coal tar, *Chemical Engineering Journal*, 266, 148-155.
- Kiss A.A., 2019, Rethinking energy use for a sustainable chemical industry, *Chemical Engineering Transactions*, 76, 13-18.
- Li W.W., Yu H.Q., He Z., 2014, Towards sustainable wastewater treatment by using microbial fuel cell-centered technologies, *Energy & Environmental Science*, 7(3), 911-924.
- Tian W.D., Wang X., Fan C.Y., Cui Z., 2019, Optimal treatment of hypersaline industrial wastewater via bipolar membrane electrodialysis, *ACS Sustainable Chemistry & Engineering*, 7, 12358-12368.
- Wang S., Xiao K., Huang X., 2019, Characterizing the roles of organic and inorganic foulants in RO membrane fouling development: The case of coal chemical wastewater treatment, *Separation and Purification Technology*, 210, 1008-1016.
- Zheng S.Q., Tang Q., He J., 2016, VFFDT: a new software for preparing AMBER force field parameters for metal-containing molecular systems, *Journal of Chemical Information and Modeling*, 56(4), 811-818.
- Zhang Y., Zhao T.S., Zhang Z.Z., Zhou A.J., Liang X.M., Wan J., Feng X.N., 2017, Modeling and dynamic assessment on sustainable development of drainage enterprise: Application of a coupled system dynamics-comprehensive assessment model, *Journal of Cleaner Production*, 141, 157-167.